International Journal of Research
Available at https://edupediapublications.org/journals
e-ISSN: 2348-6848
p-ISSN: 2348-795X
Volume 05 Issue 07
March 2018

Distributed Mechanism by Wireless Acoustic Sensor Networks with Blind Synchronization

Ch. Bharathi & Maddali M. V. M. Kumar
[#1]PG Student, Dept. of MCA, St. Ann's College of Engineering & Technology, Chirala.
[#2]Assistant Professor, Dept. of MCA, St. Ann's College of Engineering & Technology, Chirala.

ABSTRACT:*In wireless acoustic sensor systems (WASNs), testing rate balances (SROs) between hubs are inescapable, and perceived as one of the difficulties that must be settled for a sound exhibit handling. A disentangled free-space engendering is considered with a solitary wanted source impinging WASNs from the far-field and sullied by a diffuse clamor. In this paper, we break down the hypothetical execution of a settled superdirective beamformer (SDBF) in nearness of SROs. The SDBF execution misfortune because of SROs is showed as a bending of the ostensible beampattern and an overabundance clamor influence at the yield of the beamformer. We likewise propose an iterative calculation for SROs estimation.The hypothetical outcomes are approved by recreation.*

Index Terms— Blind synchronization, Wireless acoustic sensor network, Sampling rate offset

1. INTRODUCTION

The use of wireless acoustic sensor network (WASN) as a discourse handling instrument has as of late pulled in a huge research consideration. Alongside the engaging favorable circumstances offered by WASNs, some new difficulties emerge. One of the difficulties is the synchronization between WASN hubs. As opposed to a brought together receiver's cluster, where all signs are inspected with a similar clock, the testing procedure in each WASN hub depends on its neighborhood clock source, therefore, examining rate counter balances are unavoidable.

Check synchronization in disseminated sensors organize has been tended to in the writing, in a more extensive setting than discourse handling - e.g. in [1], [2]. This essential point was additionally considered when all is said in done discourse/sound handling applications, for example, re sound cancelation [3], and dazzle source partition [4]. In WASN, the synchronization strategies can be arranged in two gatherings: the time stamps approach which uses the correspondence interfaces between the sensors to convey synchronization information in the system, and a visually impaired approach which just uses the acoustic signs. Early works utilizing the time stamps approach are [5] and [2]. As of late, a complete report was exhibited in [6], where synchronization is done utilizing joined equipment and programming techniques. The visually impaired approach was likewise a subject for a lot of research [7], [8], [9], [10]. The general thought is to show the bending forced by the SRO on the sound flags and to appraise the SROs in the WASN as for (w.r.t.) an acoustical flag from a reference hub.

In the present commitment, we embrace the visually impaired approach. The SRO impact is displayed as a period fluctuating postponement between the signs. Utilizing this guess, we hypothetically examine the SDBF beam pattern and the abundance clamor control at the yield of the SDBF in nearness of SRO. Moreover, we propose an iterative calculation for SRO estimation. The calculation depends on boosting the rationality between the WASN signals, in the STFT space.

2. PROBLEM FORMULATION

Consider a WASN including M mouthpieces, going for improving a coveted discourse motion within the sight of a circularly isotropic clamor field, otherwise called diffuse commotion field. In the STFT space,

International Journal of Research
Available at https://edupediapublications.org/journals
e-ISSN: 2348-6848
p-ISSN: 2348-795X
Volume 05 Issue 07
March 2018

the discourse flag is signified s(l, k), the discourse controlling vector is meant g(k), and the commotion at the mth mouthpiece is meant vm(l, k), where l is the edge record, and k = 0, . . . , K − 1 is the recurrence file. The STFT examination window length is signified L. The discourse upgrade is refined by applying the base difference distortionless reaction (MVDR) beamformer. In the spin-off, the term ostensible will relate to values utilized for planning the beamformer. The ostensible exhibit flag is given by:

$$\mathbf{z}^{n}(l,k) = \mathbf{g}(k)s(l,k) + \mathbf{v}(l,k). \qquad (1)$$

For straightforwardness, we accept in the spin-off that every hub contains a solitary mouthpiece. Indicate the inspecting rate at the mth receiver as fs,m. Without loss of sweeping statement, the testing rate of the mth hub is characterized as far as the inspecting rate of the primary (reference) hub, fs, as fs,m = fs/am the place a1 = 1. The personality between the SRO marvel and time-scaling was presented in [9]. Utilizing this character, we can figure the genuine exhibit motion as:

$$\mathbf{z}^{n}(l,k) = \begin{bmatrix} \bar{s}_1(l,k) & 0 & \cdots \\ 0 & \ddots & 0 \\ \vdots & 0 & \bar{s}_M(l,k) \end{bmatrix} \begin{bmatrix} \bar{g}_1(k) \\ \vdots \\ \bar{g}_M(k) \end{bmatrix} + \begin{bmatrix} \bar{v}_1(l,k) \\ \vdots \\ \bar{v}_M(l,k) \end{bmatrix}, \qquad (2)$$

where s˜m(l, k) and v˜m(l, k) are the STFTs of the time-scaled, constant time, discourse and the clamor signals, s(amt) and vm(amt), separately with t indicating the consistent time hub. Also, g˜m(k) is the discrete Fourier change of the time-scaled, examined, motivation reaction between the discourse and the mth sensor gm(amt).

For effortlessness, we are thinking about a free-field situation and a straight amplifier cluster comprising of M receivers with dm being the separation between the mth mouthpiece and the reference (first) mouthpiece. In spite of the fact that we accept a direct cluster in this paper, every one of the outcomes can be promptly reached out to a discretionary three-dimensional WASN design. The discourse flag is impinging on the cluster from a far-field with a heading of arival (DOA) signified by θ. As needs be, the MVDR which is a SDBF for our situation, is exclusively characterized by the geometrical properties of the setup:

$$\mathbf{w}(k) = \frac{\mathbf{\Gamma}_{\mathbf{vv}}^{-1}(k)\mathbf{g}(k)}{\mathbf{g}^{H}(k)\mathbf{\Gamma}_{\mathbf{vv}}^{-1}(k)\mathbf{g}(k)}, \qquad (3)$$

where Γvv(k) is the spatial rationality network of the diffuse commotion with [γvv(k)]i,j = sinc 2π(di−dj) λk , λk = c fs k is the wavelength relating to the kth recurrence list, c is the sound speed in the medium, and the directing vector g(k) is given by:

$$\mathbf{g}(k) = \left[e^{-j2\pi \frac{d_1}{\lambda_k}\cos(\theta)}, \cdots, e^{-j2\pi \frac{d_M}{\lambda_k}\cos(\theta)} \right]^{T}. \qquad (4)$$

In the extent of this work we look at the execution of w(k) when connected to the unsynchronized flag z u (l, k), and propose a strategy for assessing the SROs {am} M m=2.

3. SDBF PERFORMANCE ANALYSIS WITH SRO

We swing now to the deduction of a streamlined articulation for z u (l, k). We consider the mth receiver motion as an element of the constant time tm, with time pivot tm identified with the time hub of the main mouthpiece motion by tm = amt1, and am = 1 + m is the individual SRO. The constant time tm can be characterized as far as t1, as proposed in [8]:

$$\begin{aligned} t_m &= (1+\epsilon_m)t_1 = (1+\epsilon_m)(t_1 - T_l) + (1+\epsilon_m)T_l = \\ &= t_1 - T_l + \epsilon_m(t_1 - T_l) + \epsilon_m T_l + T_l, \end{aligned} \qquad (5)$$

Where Tl is the center of the lth frame at the first microphone. Considering the lth frame, t1 is within

International Journal of Research
Available at https://edupediapublications.org/journals
e-ISSN: 2348-6848
p-ISSN: 2348-795X
Volume 05 Issue 07
March 2018

the range of Tl− L 2fs ≤ t1 ≤ Tl + L 2fs , and hence |m|(t1 −Tl) ≤ |m| L 2fs . Assuming both m and L are sufficiently small, the term m(t1 −Tl) can be neglected, resulting in:

$$t_m - T_l \approx t_1 - T_l + \epsilon_m T_l. \qquad (6)$$

Based on (6), and the properties of the STFT we can approximate the SRO effect on the speech and the noise signals in the STFT domain as follows:

$$\tilde{s}_m(l,k) \approx s(l,k)e^{j2\pi f_s \frac{k}{K}\epsilon_m T_l} = s(l,k)e^{j\pi k \epsilon_m l}, \qquad (7a)$$
$$\tilde{v}_m(l,k) \approx v_m(l,k)e^{j2\pi f_s \frac{k}{K}\epsilon_m T_l} = v_m(l,k)e^{j\pi k \epsilon_m l}, \qquad (7b)$$

While the furthest right term in (7a) and (7b) are gotten, without loss of consensus, for investigation window length of L = K, and half cover between progressive edges. For this situation, we can substitute: Tl = L 2fs l.

Consider gm(k) = e −j2π dmλk cos(θ) , the discrete Fourier change of the examined, ostensible, drive reaction between the discourse source and the mth sensor gm(t). Because of SRO, the time pivot of the drive reaction is scaled by am. While applying the discrete Fourier change to the time-scaled, and tested drive reaction, the kth recurrence file compares to a nonstop time motion with a wavelength of amλk, rather than λk in the ostensible case. A surmised articulation for g˜m(k) brings about by supplanting the term 1/am with its first-arrange Taylor arrangement guess 1 − m:

$$\tilde{g}_m(k) = e^{-j2\pi \frac{d_m}{a_m \lambda_k}\cos(\theta)} \approx \qquad (8)$$
$$\approx e^{-j2\pi \frac{d_m}{\lambda_k}\cos(\theta)} \cdot e^{j2\pi \frac{d_m}{\lambda_k}\cos(\theta)\epsilon_m}.$$

A simplified expression for z u (l, k) is obtained by substituting (7a), (7b), and (8) in (2):

$$\mathbf{z}^u(l,k) \approx \mathbf{E}_s(l,k)\mathbf{g}(k,\theta)s(l,k) + \mathbf{E}(l,k)\mathbf{v}(l,k) \qquad (9)$$

Where the SRO effect is modeled by the diagonal matrices Es(l, k) and E(l, k):

$$\mathbf{E}_s(l,k) = \begin{bmatrix} e^{j\pi\left(\frac{2d_1}{\lambda_k}\cos(\theta)+kl\right)\epsilon_1} & 0 & \cdots \\ 0 & \ddots & 0 \\ \vdots & 0 & e^{j\pi\left(\frac{2d_M}{\lambda_k}\cos(\theta)+kl\right)\epsilon_M} \end{bmatrix}, \qquad (10)$$

$$\mathbf{E}(l,k) = \begin{bmatrix} e^{j\pi kl\epsilon_1} & 0 & \cdots \\ 0 & \ddots & 0 \\ \vdots & 0 & e^{j\pi kl\epsilon_M} \end{bmatrix}. \qquad (11)$$

Consider the impact of the SRO on the shaft example of the SDBF connected to z u (l, k). The ostensible bar example of the SDBF is characterized by Bn (k, θ) = wH(k)g(k, θ). As needs be, by looking at (9) to (1), the shaft example of the ostensible beamformer w(k) connected to the unsynchronized signs is given by:

$$B(l,k,\theta) = \mathbf{w}^H(k)E_s(l,k)\mathbf{g}(k,\theta). \qquad (12)$$

Note, that the beam pattern in the unsynchronized case is timedependent, because of the floating postponement. The overabundance commotion control at the yield of the unsynchronized beamformer is characterized as:

$$R \triangleq \frac{E\{\|\mathbf{v}^{sro}\|^2\}}{E\{\|\mathbf{v}^n\|^2\}} = \frac{\mathbf{w}^H(k)\mathbf{E}(l,k)\mathbf{\Gamma}_{vv}(k)\mathbf{E}^H(l,k)\mathbf{w}(k)}{\mathbf{w}^H(k)\mathbf{\Gamma}_{vv}(k)\mathbf{w}(k)} =$$
$$= \gamma(l,k)\cdot\frac{1}{\mathbf{g}^H(k)\mathbf{\Gamma}_{vv}^{-1}(k)\mathbf{g}(k)}, \qquad (13)$$

where:

$$\gamma(l,k) = \mathbf{g}^H(k)\mathbf{\Gamma}_{vv}^{-1}(k)\mathbf{E}(l,k)\mathbf{\Gamma}_{vv}(k)\mathbf{E}^H(l,k)\mathbf{\Gamma}_{vv}^{-1}(k)\mathbf{g}(k). \qquad (14)$$

In conclusion, the beampattern of w(k) applied to z u (l, k), and the excess noise power due to SROs are given by equations (12) and (13), respectively.

4. EXPERIMENTAL STUDY

In this area we confirm the strategies proposed in Sec. 3. For that reason, a simulative benchmark has been composed. Two simulative investigations were done. The first is going for checking the SDBF pillar design, and the overabundance clamor control

International Journal of Research
Available at https://edupediapublications.org/journals
e-ISSN: 2348-6848
p-ISSN: 2348-795X
Volume 05 Issue 07
March 2018

models inferred in [10], separately. The second investigation is going for breaking down the execution of the SRO estimation calculation.

4.1. SRO effect on SDBF

In this examination, a uniform straight cluster with M = 4 amplifiers divided by 11 cm was utilized. A discourse flag impinging on the exhibit from the far-field with DOA equivalent to θ = 600 is recreated in a commotion free condition. The unsynchronized signs were created by re-examining the synchronized signs with arbitrarily chose SROs, meant SROm, for m = 2, . . . , M. The normal SRO is indicated SRO = 1 M−1 PM m=2 SROm. The cluster pick up towards an unsynchronized flag touching base from 0 ≤ θ ≤ 1800 was figured as a power proportion of the flag at the yield of the SDBF and the flag of one of the mouthpieces. This experimental pick up is signified by Bsim.

An examination amongst Bsim(θ) and B(θ) as characterized by (12) is displayed in Fig. 1. Obviously, the diagnostically determined beam pattern is in a decent concurrence with the observational one. The impact of the beam pattern variety in time is additionally exemplified in Fig. 1, by looking at the upper and the lower figures. The ostensible beam pattern of the SDBF Bn and the normal (after some time) beam pattern B because of SRO = 100 PPM are likewise delineated in the two figures in Fig. 1.

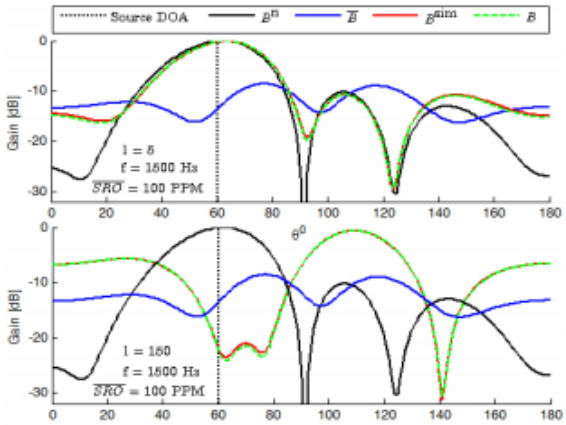

Fig. 1. Empirical vs. analytical beampatterns of SDBF

The affectability of the SDBF to SROs is investigated in Fig. 2. As observed from the upper figure, the normal beam pattern because of SRO = 1 PPM is sensibly like the ostensible one. Be that as it may, the normal beam pattern because of an unassuming blemish of SRO = 10 PPM is a long way from the ostensible one, as appeared in the base plot. Note that, the level of the SRO influence the rate at which the beam pattern fluctuates. In any case, notwithstanding for the littlest SRO, sufficiently after time has slipped by the beam pattern will be altogether different from the ostensible one.

To assess the abundance commotion control display, a diffuse clamor v n (l, k) was created by the technique proposed in [10]. SROs with SRO = 100 PPM were acquainted with the synchronized clamor signals, bringing about v u (l, k). The exact overabundance commotion control Rsim was figured as the power proportion between SDBF reaction to v n (l, k) and SDBF reaction to v u (l, k). A correlation amongst Rsim and R as characterized by (13) is compressed in Table 1. It is fascinating to take note of that the commotion lessening at a high recurrence is relatively unaffected by the SRO. This is because of the normal for the diffuse clamor, which is known to end up plainly confused at higher frequencies [10], and thus its decrease isn't influenced by the SRO. Despite what might be expected, the commotion diminishment at low frequencies is corrupting with time.

International Journal of Research
Available at https://edupediapublications.org/journals
e-ISSN: 2348-6848
p-ISSN: 2348-795X
Volume 05 Issue 07
March 2018

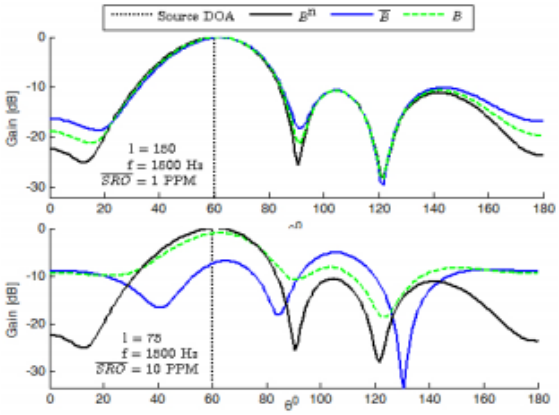

Fig. 2: SDBF beam patterns for various SROs

f[Hz]	l	R^{sim}[dB]	R[dB]
300	5	2	1
1500	5	0.3	0
300	150	16	18
1500	150	−0.4	0

Table 1: Analytical and empirical excess noise power at the output of the SDBF

4.2. Iterative estimation of SRO

In this piece of the work, we are assessing the proposed SRO estimation system (18). The test setup is like the one portrayed in Sec. 5.1, with a special case of both diffused commotion, and discourse flag being all the while exhibit. The flag to commotion proportion (SNR) was set to 10 dB. In the continuation we talk about the SRO estimation for the second mouthpiece (m = 2) for instance. Comparable strategy can be connected to any receiver m = 2, . . . , M. The SRO was set to 100 PPM. The investigation window is set to L = 1024, and LJ = 150 casings were utilized for evaluating the SRO.

The execution of the slope Acescent technique is portrayed in Figs. 3 and 4. It is promptly watched that the cost work |J2(k, 2)| 2 is, all in all, non-curved. Consequently, joining of (18) to the worldwide most extreme can't be ensured. In reality, the strategy is caught in a nearby most extreme because of poor instatement, as appeared in Fig. 3.

An effective estimation of 2 is portrayed in Fig. 4. It is effortlessly confirmed that the cost work is getting smoother when a lower recurrence band is considered, which encourages sufficient estimation execution in this illustration. It ought to be

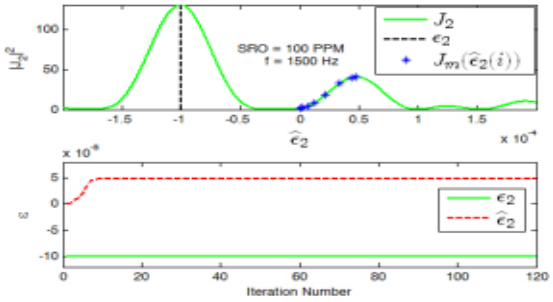

Fig. 3. Gradient Acescent trapped in a local maximum due to poorly chosen initial conditions.

Noticed that the slant of the cost work is getting moderate once a low recurrence band is considered, which additionally hampers the estimation execution. The above perceptions direct that a legitimate recurrence choice philosophy is required with a specific end goal to effectively gauge the SROs utilizing the proposed iterative technique. Be that as it may, such a procedure is past the extent of the present commitment and will be a subject for a future report.

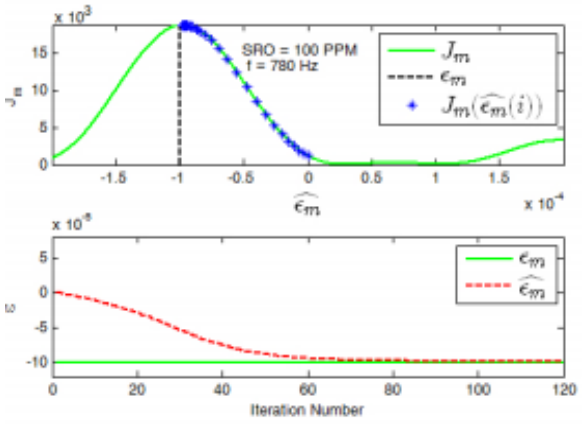

Fig. 4. Cost function |J2| 2 and the Gradient Acescent learning curve.

5. CONCLUSION

Synchronization between WASN hubs is considered in this work. The SDBF execution misfortune because of SRO is showed as a bending of the ostensible beampattern and an abundance clamor influence at the yield of the beamformer. An iterative strategy for SROs estimation was proposed. The strategies and methods introduced wereapproved by reproductions and their impediments were exemplified.

REFERENCES

[1] Yik-Chung Wu, QasimChaudhari, and ErchinSerpedin, "Clock synchronization of wireless sensor networks," IEEE Signal Processing Magazine, vol. 28, no. 1, pp. 124–138, 2011.

[2] Luca Schenato and Federico Fiorentin, "Average timesync: A consensus-based protocol for time synchronization in wireless sensor networks," in Estimation and Control of Networked Systems, 2009, vol. 1, pp. 30–35.

[3] Matthias Pawig, Gerald Enzner, and Peter Vary, "Adaptive sampling rate correction for acoustic echo control in voice-over-IP," IEEE Transactions on Signal Processing, vol. 58, no. 1, pp. 189–199, 2010.

[4] Stefan Wehr, Igor Kozintsev, Rainer Lienhart, and Walter Kellermann, "Synchronization of acoustic sensors for distributed ad-hoc audio networks and its use for blind source separation," in the 6th IEEE International Symposium on Multimedia Software Engineering, 2004, pp. 18–25.

[5] Raj ThilakRajan and Alle-Jan van der Veen, "Joint ranging and clock synchronization for a wireless network," in the 4th IEEE International Workshop on Computational Advances in Multi-Sensor Adaptive Processing (CAMSAP), 2011, pp. 297–300.

[6] JoergSchmalenstroeer, Patrick Jebramcik, and Reinhold Haeb-Umbach, "A combined hardware–software approach for acoustic sensor network synchronization," Signal Processing, vol. 107, pp. 171–184, 2015.

[7] ShmulikMarkovich-Golan, Sharon Gannot, and Israel Cohen, "Blind sampling rate offset estimation and compensation in wireless acoustic sensor networks with application to beamforming," in International Workshop on Acoustic Signal Processing (IWAENC), 2012.

[8] Shigeki Miyabe, Nobutaka Ono, and Shoji Makino, "Blind compensation of inter-channel sampling frequency mismatch with maximum likelihood estimation in STFT domain," in IEEE International Conference on Acoustics, Speech and Signal Processing (ICASSP), 2013, pp. 674–678.

[9] Dani Cherkassky and Sharon Gannot, "Blind synchronization in wireless sensor networks with application to speech enhancement," in the 14th International Workshop on Acoustic Signal Enhancement (IWAENC), 2014, pp. 183–187.

[10] J. Babichaitanya, Maddali M.V.M. Kumar, "Secured System for Keylogging – Resilient Virtual Validation," in International Journal of Advanced Research in Computer Science and Software Engineering, 2015, pp. 691-695.

[11] Emanuel A.P. Habets and Sharon Gannot, "Generating ¨ sensor signals in isotropic noise fields," The Journal of the Acoustical Society of America, vol. 122, no. 6, pp. 3464–3470, 2007.

ABOUT AUTHORS:

e-ISSN: 2348-6848
p-ISSN: 2348-795X
Volume 05 Issue 07
March 2018

Ch. Bharathi is currently pursuing her MCA in MCA Department, St. Ann's College Engineering and Technology,Chirala A.P. She received her Bachelor of Science from ANU.

Mr. Maddali M. V. M. Kumar received his Master of Technology in Computer Science & Engineering from JNTUK and currently pursuing his Ph.D. in Computer Science & Engineering from ANU. He is working as an Assistant Professor in the Department of MCA, St. Ann's College of Engineering & Technology. He is a Life Member in CSI & ISTE. His research focuses on the Computer Networks, Mobile & Cloud Computing.